Article

Temperature and Particle Size Influence on the High Cycle Fatigue Behavior of the SiC Reinforced 2124 Aluminum Alloy

Lisa Winter *, Kristin Hockauf and Thomas Lampke [iD]

Institute of Materials Science and Engineering, Technische Universität Chemnitz, Erfenschlager Str. 73, 09125 Chemnitz, Germany; kristin.hockauf@mb.tu-chemnitz.de (K.H.); thomas.lampke@mb.tu-chemnitz.de (T.L.)

* Correspondence: lisa.winter@mb.tu-chemnitz.de; Tel.: +49-371-531-32632

Abstract: In this work the high cycle fatigue behavior of a particulate reinforced 2124 aluminum alloy, manufactured by powder metallurgy, is investigated. SiC particles with a size of 3 μm and 300 nm and a volume fraction of 5 and 25 vol %, respectively, were used as reinforcement component. The present study is focused on the fatigue strength and the influence of particle size and temperature. Systematic work is done by comparing the unreinforced alloy and the reinforced conditions. All of the material conditions are characterized by electron microscopy and tensile and fatigue testing at room temperature and at 180 °C. With an increase in temperature the tensile and the fatigue strength decrease, regardless of particle size and volume fraction due to the lower matrix strength. The combination of 25 vol % SiC particle fraction with 3 μm size proved to be most suitable to achieve a major fatigue performance at room temperature and at 180 °C. The fatigue strength is increased by 40% when compared to the unreinforced alloy, as it is assumed the interparticle spacing for this condition reaches a critical value then.

Keywords: metal matrix composite; high cycle fatigue; high temperature properties; particulate reinforcement; aluminum alloy

1. Introduction

The performance requirements of materials for advanced engineering applications in the aerospace and automotive industry call for lightweight structural composite materials. Aluminum matrix composites (AMCs) are designed to meet these requirements such as a high specific strength and stiffness [1–3], an excellent fatigue performance [4–7], and an enhanced thermal stability [8–10].

The mechanical properties and the fatigue performance of the AMCs are strongly determined by different factors. Composites processed by powder metallurgy, as used in this study, exhibit a homogeneous particle distribution, and therefore superior mechanical properties and an outstanding fatigue performance when compared to other manufacturing processes [11]. Tensile strength and fatigue resistance of the composites are also strongly influenced by the aging condition and the matrix microstructure [12,13]. Particle shape [14,15], particle size, and volume fraction [16–20] are critical factors for the mechanical properties and fatigue behavior of the AMCs. Due to an enhanced load transfer from the softer matrix to the stiffer particles, an increase in particle volume fraction and a decrease in particle size lead to a significant increase in fatigue strength [4–7,21]. Further, particle size and interparticle spacing are determining factors for the fracture behavior [22,23]. At room temperatures, decohesion of the particles from the matrix is unlikely to occur, due to the high interface strength. Therefore, the probability of particle failure increases [21,24]. Larger particles provide a minor resistance against particle failure [4,15,25] and fatigue cracks initiate preferably at them due

to the higher local stress concentration [12,17,26]. In contrast, for composites with smaller particles, the stress distribution is more homogeneous due to minor local stress concentrations and smaller interparticle spacing [27]. With increasing temperature, interface decohesion is generally more likely to occur, but larger particles are still prone to fracture [28–30].

As a result, to enhance the fatigue limit and minimize critical factors for crack initiation, the usage of small particles is required. Nonetheless, there is only limited data in literature on particle sizes smaller than 5 μm. Therefore, the purpose of the present study is to examine the influence of particles with 3 μm and 300 nm size with two different particle volume fractions. The fatigue tests were carried out at room temperature and 180 °C and the effects of temperature and particle size on the fatigue strength are discussed.

2. Materials and Methods

2.1. Material

In this study a 2124 aluminum alloy reinforced with two different particle volumes and particle sizes, respectively, was investigated. The material conditions were processed by high energy ball milling, hot isostatic pressing and forging by Materion Aerospace Composites AMC (Farnborough, UK) and were provided as plates with the dimensions given in Figure 1. The chemical composition of the matrix material is given in Table 1. SiC particles with 3 μm and 300 nm size were used as reinforcement. In this study, five material conditions were investigated: Unreinforced, reinforced with 5 vol % and 25 vol % 3 μm SiC particles and reinforced with 5 vol % and 25 vol % 300 nm SiC particles. All of the tested conditions were solid-solution treated at 505 °C for 60 min, and subsequently cold-aged at room temperature (RT) for 100 h.

Table 1. Chemical composition of the 2124 aluminum powder alloy.

Element	Al	Cu	Mg	Mn	Si	Fe	Cr	Ti	Zn	Others
wt %	91.25	4.9	1.8	0.9	0.2	0.3	0.1	0.15	0.25	0.15

2.2. Methods of Mechanical Testing and Electron Microscopy

Quasi-static tensile tests were performed in a Zwick-Roell servohydraulic testing machine (Zwick, Ulm, Germany) at a strain rate of $10^{-3} \cdot s^{-1}$ at room temperature and at 180 °C. For tensile testing cylindrical specimens were used with a cross section of 3.5 mm and a gauge length of 10.5 mm (sample orientation is given in Figure 1). For each condition, three samples were tested.

High cycle fatigue tests were performed on a RUMUL Testronic resonant testing machine (Russenberger Prüfmaschinen AG, Neuhausen am Rheinfall, Switzerland) under tension-tension loading with a load ratio of $R = 0.1$. The fatigue tests were carried out until the endurance limit of $N_D = 10^7$ cycles (approx. 27 h testing time) was reached or until a crack occurred, which was detected by a drop in the resonant frequency of 2 Hz or more. Axial fatigue specimens with 4.0 mm minimum diameter were used for fatigue testing (sample orientation and specimen geometry are given in Figure 1). For testing at 180 °C, the tensile and fatigue specimens were preheated for 30 min at this temperature. This led to a further aging of the formerly underaged matrix.

From all of the conditions, samples for microstructural analysis were extracted from the forged material, as shown in Figure 1. These samples were analyzed by quadrant back scatter diffraction (QBSD) at 20 kV using a Zeiss Neon 40 field emission microscope (Carl Zeiss MicroImaging GmbH, Jena, Germany).
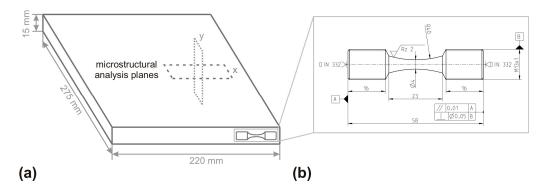
Figure 1. Schematic figure of the dimensions of the forged plate, the sample orientation of the axial specimens for tensile and fatigue testing and the investigated planes for the microstructural analysis (**a**) and the specimen geometry for fatigue testing (**b**).

3. Results and Discussion

3.1. Microstructure

All of the tested material conditions exhibit a homogeneous microstructure with numerous coarse Al_2Cu precipitates. The reinforced conditions show areas without reinforcement components with a width of 30–150 μm and a height of about 10–20 μm (see Figure 2). The particle distribution is rather homogeneous for all reinforced conditions. The SiC particles are irregularly shaped and exhibit an intact interface to the aluminum matrix (see Figure 3).
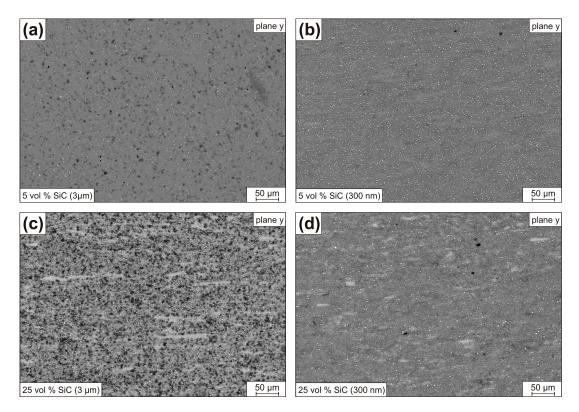

Figure 2. Quadrant back scatter diffraction (QBSD) micrographs of the 2124 aluminum alloy reinforced with (**a**,**b**) 5 vol % and (**c**,**d**) 25 vol % SiC particles with a size of (**a**,**c**) 3 μm and (**b**,**d**) 300 nm. The reinforced conditions exhibit areas without reinforcement component (matrix is light grey, particles are dark grey, Al_2Cu precipitates are white).
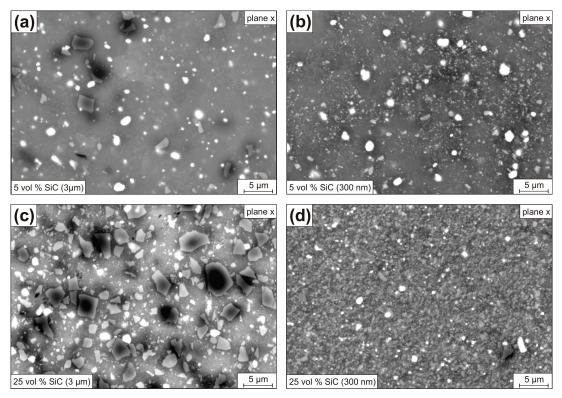
Figure 3. QBSD micrographs of the 2124 aluminum alloy reinforced with (**a**,**b**) 5 vol % and (**c**,**d**) 25 vol % SiC particles with a size of (**a**,**c**) 3 μm and (**b**,**d**) 300 nm. The SiC particles are irregularly shaped and finely dispersed: Matrix and particles exhibit an intact interface.

3.2. Tensile Testing

In Figure 4 and Table 2 the tensile properties for all of the tested material conditions (in underaged heat treatment condition) and temperatures are given. At room temperature, the unreinforced alloy exhibits the lowest yield strength with 341 MPa, as well as the highest uniform elongation with 17%, and therefore the highest ductility for the tested material conditions (see Figure 4a). The presence of a 5% volume fraction of reinforcement decreases the uniform elongation by approximately a third. For 25 vol % SiC particles, the uniform elongation is drastically reduced to only 1%. For 5 vol % particle fraction, a reduction in particle size from 3 μm to 300 nm increases the yield strength by 5% to 378 MPa. The strengthening effect caused by particle size reduction is more pronounced for 25 vol % particle fraction, as the yield strength for the material with 300 nm particles is increased by 38% to 633 MPa, which is the highest yield strength of all tested material conditions. This is an increase by 85% compared to the unreinforced alloy. Clearly, for the reinforced material the determining factor for the elongation is the reinforcement volume fraction, whereas both particle size and volume fraction determine the strength.

The increase in strength due to the particulate reinforcement is caused mainly by the load transfer from the matrix to the stiffer reinforcement component [7,23]. Further, dispersion strengthening occurs, which leads to two main mechanisms. Dislocation generation and the high dislocation density due to the difference in the thermal expansion coefficient of the matrix and the SiC particle [31], as well as the impediment of the dislocation movement due to the high dislocation density and the reinforcement component [4,12] act as strengthening mechanisms. An increase in particle volume fraction and a decrease in particle size lead to an enhancement of this effect, and therefore to a further increase in strength and a decrease in ductility [1,32]. The minor ductility of the reinforced material and the further decrease with an increase in particle volume fraction is caused by the major residual stresses induced by the reinforcement component [27].

At 180 °C all of the material conditions exhibit a decrease in strength and an increase in ductility when compared to the room temperature properties (see Figure 4b). The unreinforced alloy exhibits

the lowest yield strength with 282 MPa and the highest uniform elongation with approximately 18%. At 180 °C the influence of particle size on the yield strength decreases. The reinforced material with 5 vol % particle fraction exhibit only an 18% higher yield strength if compared to the unreinforced alloy. Reinforcement with 25 vol % leads to the highest yield strength of about 420 MPa, which is twice as high as for the unreinforced alloy. At 180 °C, smaller particle sizes result in a higher ductility. The elongation to failure is at least one third higher in the material with smaller reinforcements, than in the material with 3 mm particles. Clearly, the uniform elongation for 5 vol % particle fraction and both particle sizes is nearly the same as at room temperature.
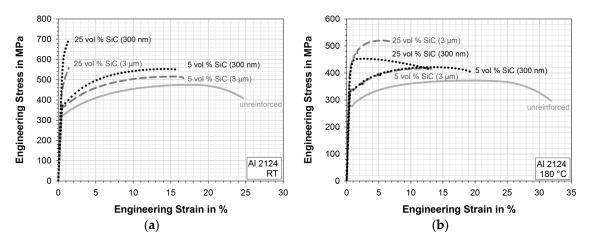

Figure 4. Tensile behavior of the unreinforced and reinforced 2124 aluminum alloy (**a**) at room temperature and (**b**) at 180 °C. Figure shows one representative curve for each condition.

Table 2. Mechanical properties determined by tensile testing of the unreinforced and reinforced 2124 aluminum alloy. The deviation is given in absolute values.

Condition of the 2124 Aluminum Alloy	Temperature	Yield Strength in MPa	Ultimate Tensile Strength in MPa	Uniform Elongation in %	Elongation to Failure in %
unreinforced	RT	341 ± 35	471 ± 8	16.7 ± 1.0	24.8 ± 1.1
5 vol % SiC (3 µm)	RT	358 ± 8	508 ± 9	14.0 ± 1.0	15.6 ± 0.8
25 vol % SiC (3 µm)	RT	460 ± 6	573 ± 62	1.5 ± 1.2	1.5 ± 1.2
5 vol % SiC (300 nm)	RT	378 ± 1	552 ± 1	13.3 ± 1	14.5 ± 1.0
25 vol % SiC (300 nm)	RT	633 ± 10	727 ± 33	1.0 ± 0.4	1.0 ± 0.4
unreinforced	180 °C	282 ± 15	380 ± 17	17.4 ± 1.6	28.1 ± 3.1
5 vol % SiC (3 µm)	180 °C	332 ± 4	413 ± 4	11.9 ± 0.5	13.5 ± 1.0
25 vol % SiC (3 µm)	180 °C	426 ± 6	529 ± 11	4.7 ± 0.4	6.0 ± 1.6
5 vol % SiC (300 nm)	180 °C	337 ± 5	423 ± 5	12.5 ± 0.3	18.8 ± 1.6
25 vol % SiC (300 nm)	180 °C	419 ± 4	458 ± 5	2.0 ± 0.3	13.1 ± 1.2

With an increasing temperature, the matrix properties become of more influence for the tensile properties and the strength decreases, regardless of the particle volume fraction and the particle size [33]. The influence of particle size on the strength decreases due to the softening of the overaged matrix and the increase in relaxation of residual stresses and local stress concentration [30]. The probability for particle fracture decreases and matrix failure near the interface or interfacial decohesion becomes more prominent [29,34]. The ductility for reinforced material with smaller particles is increased due to their smaller interparticle spacing, and therefore a more homogeneous distribution of the plastic strain in the matrix [27,30].

3.3. High Cycle Fatigue Behavior

The high cycle fatigue behavior of the tested material conditions and its dependence on temperature is shown in Figure 5 and the fatigue strength for $N_D = 10^7$ cycles is listed in Table 3.

At room temperature, the unreinforced alloy exhibits a fatigue strength of 280 MPa (see Figure 5a). The fatigue strength of both 5 vol % reinforced conditions is smaller than for the unreinforced alloy. The condition with 3 μm particle size exhibits the lowest fatigue strength with 250 MPa. Reinforcement with 25 vol % 3 μm SiC particles increases the fatigue strength by 40% if compared to the unreinforced alloy. Reducing the particle size to 300 nm leads to an additional increase by 6%, and therefore to the highest fatigue strength of all conditions with 410 MPa.
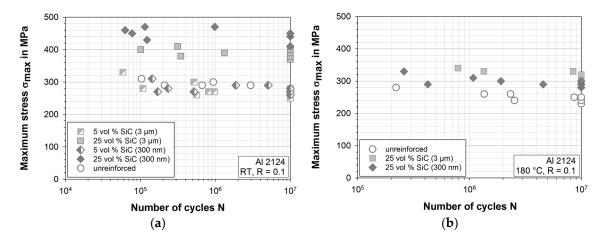

Figure 5. High cycle fatigue behavior of the unreinforced and reinforced 2124 aluminum alloy at $R = 0.1$ and (**a**) at room temperature and (**b**) at 180 °C.

Table 3. Fatigue limit at $N_D = 10^7$ cycles of the unreinforced and reinforced 2124 aluminum alloy at RT and load ratio $R = 0.1$.

Condition of the 2124 Aluminum Alloy	Temperature	Maximum Stress σ_{max} in MPa	Reduction in Fatigue Limit in % [1]	Increase in Fatigue Limit in % [2]
Unreinforced	RT	280	-	-
5 vol % SiC (3 μm)	RT	250	10.7	-
25 vol % SiC (3 μm)	RT	390	-	39.3
5 vol % SiC (300 nm)	RT	270	3.6	-
25 vol % SiC (300 nm)	RT	410	-	46.4
Unreinforced	180 °C	230	17.9	-
25 vol % SiC (3 μm)	180 °C	320	-	39.1
25 vol % SiC (300 nm)	180 °C	280	-	21.7

[1] referring to the unreinforced alloy at room temperature. [2] referring to the unreinforced alloy at the respective temperature.

A high yield and tensile strength of the particle reinforced material do not necessarily result in a high fatigue strength [6]. A deteriorated fatigue performance of the composites in comparison to the unreinforced alloy can be explained by a high defect density, particle clustering, or a high porosity of the material [7,35]. As these effects were not noticeable for the investigated conditions, the minor fatigue strength of the reinforced conditions with 5 vol % particle fraction is attributed to the local stress raisers induced by the reinforcement component. This diminishes the beneficial strengthening effect of the reinforcement. The minimal fatigue strength of the reinforced condition with 5 vol % and 3 μm particles can be explained by the further increase of the local stress intensity at the particle-matrix-interface with an increase in particle size [26]. Also, the particle shape essentially affects the stress concentration [14]. Sharp edges of the irregularly shaped particles and slight imperfections of the particle surface cause a significant increase in the internal stresses. Therefore, an early formation of initial cracks can further be a reason for the minor fatigue strength of the reinforced conditions with 5 vol % particle fraction [21]. The increase in fatigue strength with an increase in particle volume content and a decrease in particle

size is a well known effect [4–7,21]. An increase in volume fraction enables a higher load transfer from the matrix to the stiffer reinforcement component [6,7]. An additional decrease in particle size leads to a decrease in the interparticle spacing, which prevents the formation of reversible slip bands when a critical value is reached [5].

In Figure 5b, the high cycle fatigue behavior at 180 °C is shown. The reinforced conditions with 5 vol % SiC particles were not tested at this temperature due to their minor fatigue performance at room temperature. Due to the long testing time, overaging processes occur as observed for the tensile tests. It is assumed, that all of the tested material conditions are equally overaged after preheating for 30 min. An increase in temperature leads for the unreinforced alloy and the reinforced material to a decrease in fatigue strength. The fatigue strength of the unreinforced alloy is 230 MPa, and therefore 18% lower than at room temperature. In contrast to fatigue at room temperature, the condition with 25 vol % and 3 µm particle size exhibits the highest fatigue strength with 320 MPa, which is an increase by 40% if compared to the unreinforced alloy at 180 °C. Reinforcement with 300 nm particles leads to a much smaller increase in fatigue strength by 22%.

At higher temperatures the stress concentrations and the influence of processing defects decreases and the matrix becomes the determining factor for the fatigue strength [7,33]. The lower matrix strength, due to the overaging during testing, causes a general reduction in fatigue strength for all of the tested conditions at 180 °C [12]. Fatigue crack initiation in the matrix is the primary failure mechanism [7,20,23,36]. With increasing temperature, decohesion between the particle and the matrix is enhanced and cracks are easily initiated [28,37]. Additionally, cracks are also generated by cyclic slip deformation for reinforced conditions with a particle size smaller 20 µm [33,36]. The crack initially propagates along a slip band and ahead of the crack tip microcracking and void formation in the matrix occur [37]. These microcracks join the main crack by matrix microvoid coalescence [23,37]. In addition, the plastic zone ahead of the fatigue crack front is larger than the average interparticle spacing and determines the fracture mechanisms [37]. The findings of [33], which state a declining influence of the particle volume fraction and of the particle size on the fatigue strength with increasing temperature, could not be fully confirmed by our work. Reinforcement with 300 nm particles led to a minor increase in fatigue strength in comparison to room temperature. This effect can be explained by the relieved dislocation cross slip motion with an increased temperature due to the small interparticle spacing. Additionally, the small interparticle spacing and the high particle volume fraction lead to a major amount of particles incorporated in the plastic zone ahead of the crack tip, and therefore to major void formation. In contrast, the interparticle spacing between the 3 µm particles is large enough to impede the dislocation movement and still small enough to limit the void growth [23]. It is suggested that 3 µm is an optimal value for the particle size at the given particle fraction of 25 vol % to maximize the matrix and fatigue strength. This explains the 40% higher fatigue strength of this condition if compared to the unreinforced alloy at room temperature and 180 °C. For the commonly used minimal particle size of 5 µm, the interparticle spacing is already large enough to enable void growth and dislocation slip motion between the particles. Therefore, the strengthening effect due to particle reinforcement is smaller at higher temperatures.

4. Conclusions

The influence of temperature and particle size on the high cycle fatigue behavior of the particulate reinforced 2124 aluminum alloy is investigated. SiC particles with 3 µm and 300 nm size and a volume fraction of 5 and 25 vol %, respectively, were used as reinforcement component. The tensile properties and the fatigue behavior of the unreinforced alloy and the four reinforced conditions were compared at room temperature and at 180 °C. Conclusions can be drawn as follows:

1. Generally, the tensile and the fatigue strength of the unreinforced and the reinforced material decrease with an increase in temperature. This is attributed to the increasing influence of the lower matrix strength, regardless of the particle volume fraction and the particle size.

2. Particulate reinforcement leads to an increase in tensile strength and a loss in ductility. A high particle volume fraction enhances this effect. At room temperature, a decrease in particle size leads to a further increase in tensile strength, whereas at 180 °C, the tensile strength is not affected by a decreased particle size, nevertheless, the ductility increases.

3. The room temperature fatigue strength of the reinforced conditions with 5 vol % SiC in 3 μm and 300 nm size was minor in comparison to the unreinforced alloy. Supposedly the local stress concentrations induced by the reinforcement component lead to an early formation of initial cracks.

4. The beneficial effect of an increased particle volume fraction and a decreased particle size on the fatigue strength could be confirmed for room temperature. The condition with 25 vol % particle fraction and 300 nm size exhibited the highest fatigue strength. Whereas, at 180 °C, reinforcement with 25 vol % SiC particles leads also to a significant increase in fatigue strength when compared to the unreinforced alloy, but the percentage increase was minor for the 300 nm particles if compared to the 3 μm particles.

5. The combination of 25 vol % SiC particle fraction with 3 μm size proved to be most suitable for a major fatigue performance at room temperature and at 180 °C. It is assumed, that the interparticle spacing for this combination of particle size and fraction is large enough to impede dislocation movement and still small enough to limit void formation. Therefore, the fatigue strength was improved by 40% in comparison to the unreinforced alloy at both testing temperatures.

Author Contributions: Lisa Winter designed, performed and analyzed the experiments and is the primary author of the paper. Kristin Hockauf discussed the results and analysis with the author. Thomas Lampke supervised the work.

Conflicts of Interest: The authors declare no conflict of interest.

References

1. Doel, T.J.A.; Bowen, P. Tensile properties of particulate-reinforced metal matrix composites. *Compos. Part A Appl. Sci. Manuf.* **1996**, *27*, 655–665. [CrossRef]

2. Ceschini, L.; Morri, A.; Cocomazzi, R.; Troiani, E. Room and high temperature tensile tests on the AA6061/10vol.%Al_2O_3p and AA7005/20vol.%Al_2O_3p composites. *Mater. Sci. Eng. Technol.* **2003**, *34*, 370–374. [CrossRef]

3. Ceschini, L.; Minak, G.; Morri, A. Tensile and fatigue properties of the AA6061/20vol.% Al_2O_3p and AA7005/10vol.% Al_2O_3p composites. *Compos. Sci. Technol.* **2006**, *66*, 333–342. [CrossRef]

4. Hall, J.N.; Jones, J.W.; Sachdev, A.K. Particle size, volume fraction and matrix strength effects on fatigue behavior and particle fracture in 2124 aluminum-SiCp composites. *Mater. Sci. Eng. A* **1994**, *183*, 69–80. [CrossRef]

5. Chawla, N.; Andres, C.; Jones, J.W.; Allison, J.E. Effect of SiC volume fraction and particle size on the fatigue resistance of a 2080 Al/SiC composite. *Metall. Mater. Trans. A* **1998**, *29*, 2843–2854. [CrossRef]

6. Chawla, N.; Allison, J.E. Fatigue of Particle Reinforced Materials. In *Encyclopedia of Materials: Science and Technology*, 2nd ed.; Elsevier: Amsterdam, The Netherlands, 2001; pp. 2967–2971.

7. Llorca, J. Fatigue of particle-and whisker-reinforced metal-matrix composites. *Prog. Mater. Sci.* **2002**, *47*, 283–353. [CrossRef]

8. Furukawa, M.; Wang, J.; Horita, Z.; Nemoto, M.; Ma, Y.; Langdon, T.G. An investigation of strain hardening and creep in an Al-6061/Al_2O_3 metal matrix composite. *Metall. Mater. Trans. A* **1995**, *26*, 633–639. [CrossRef]

9. Li, Y.; Langdon, T.G. Creep behavior of an Al-6061 metal matrix composite reinforced with alumina particulates. *Acta Mater.* **1997**, *45*, 4797–4806. [CrossRef]

10. Tjong, S.C.; Ma, Z.Y. The high-temperature creep behaviour of aluminium-matrix composites reinforced with SiC, Al_2O_3 and TiB_2 particles. *Compos. Sci. Technol.* **1997**, *57*, 697–702. [CrossRef]

11. Park, B.G.; Crosky, A.G.; Hellier, A.K. High cycle fatigue behaviour of microsphere Al$_2$O$_3$–Al particulate metal matrix composites. *Compos. Part B Eng.* **2008**, *39*, 1257–1269. [CrossRef]

12. Chawla, N.; Habel, U.; Shen, Y.-L.; Andres, C.; Jones, J.W.; Allison, J.E. The Effect of Matrix Microstructure on the Tensile and Fatigue Behavior of SiC Particle-Reinforced 2080 Al Matrix Composites. *Metall. Mater. Trans. A* **2000**, *31*, 531–540. [CrossRef]

13. Srivatsan, T.S.; Mattingly, J. Influence of heat treatment on the tensile properties and fracture behaviour of an aluminium alloy-ceramic particle composite. *J. Mater. Sci.* **1993**, *28*, 611–620. [CrossRef]

14. Romanova, V.A.; Balokhonov, R.R.; Schmauder, S. The influence of the reinforcing particle shape and interface strength on the fracture behavior of a metal matrix composite. *Acta Mater.* **2009**, *57*, 97–107. [CrossRef]

15. Zhang, P.; Li, F. Effect of particle characteristics on deformation of particle reinforced metal matrix composites. *Trans. Nonferrous Met. Soc. China* **2010**, *20*, 655–661. [CrossRef]

16. Xue, Z.; Huang, Y.; Li, M. Particle size effect in metallic materials: A study by the theory of mechanism-based strain gradient plasticity. *Acta Mater.* **2002**, *50*, 149–160. [CrossRef]

17. Huang, M.; Li, Z. Size effects on stress concentration induced by a prolate ellipsoidal particle and void nucleation mechanism. *Int. J. Plast.* **2005**, *21*, 1568–1590. [CrossRef]

18. Köhler, L.; Hockauf, K.; Lampke, T. Influence of Particulate Reinforcement and Equal-Channel Angular Pressing on Fatigue Crack Growth of an Aluminum Alloy. *Metals (Basel)* **2015**, *5*, 790–801. [CrossRef]

19. Shyong, J.H.; Derby, B. The deformation characteristics of SiC particulate-reinforced aluminium alloy 6061. *Mater. Sci. Eng. A* **1995**, *197*, 11–18. [CrossRef]

20. Shin, C.S.; Huang, J.C. Effect of temper, specimen orientation and test temperature on the tensile and fatigue properties of SiC particles reinforced PM 6061 Al alloy. *Int. J. Fatigue* **2010**, *32*, 1573–1581. [CrossRef]

21. Papakyriacou, M.; Mayer, H.; Stanzl-Tschegg, S.; Groschl, M. Fatigue properties of Al$_2$O$_3$-particle-reinforced 6061 aluminium alloy in the high-cycle regime. *Int. J. Fatigue* **1996**, *18*, 475–481. [CrossRef]

22. Kamat, S.V.; Hirth, J.P.; Mehrabian, R. Mechanical properties of particulate-reinforced aluminum-matrix composites. *Acta Metall.* **1989**, *37*, 2395–2402. [CrossRef]

23. Milan, M.T.; Bowen, P. Tensile and Fracture Toughness Properties of SiC$_p$ Reinforced Al Alloys: Effects of Particle Size, Particle Volume Fraction, and Matrix Strength. *J. Mater. Eng. Perform.* **2004**, *13*, 775–783. [CrossRef]

24. Flom, Y.; Arsenault, R.J. Interfacial bond strength in an aluminium alloy 6061-SiC composite. *Mater. Sci. Eng.* **1986**, *77*, 191–197. [CrossRef]

25. Mummery, P.; Derby, B. The influence of microstructure on the fracture behaviour of particulate metal matrix composites. *Mater. Sci. Eng. A* **1991**, *135*, 221–224. [CrossRef]

26. Tokaji, K.; Shiota, H.; Kobayashi, K. Effect of particle size on fatigue behaviour in SiC particulate-reinforced aluminium alloy composites. *Fatigue Fract. Eng. Mater. Struct.* **1999**, *22*, 281–288. [CrossRef]

27. Bouafia, F.; Serier, B.; Bouiadjra, B.A.B. Finite element analysis of the thermal residual stresses of SiC particle reinforced aluminum composite. *Comput. Mater. Sci.* **2012**, *54*, 195–203. [CrossRef]

28. Hadianfard, M.J.; Healy, J.; Mai, Y.-W. Temperature effect on fracture behaviour of an alumina particulate-reinforced 6061-aluminium composite. *Appl. Compos. Mater.* **1994**, *1*, 93–113. [CrossRef]

29. Poza, P.; Llorca, J. Fracture toughness and fracture mechanisms of Al-Al$_2$O$_3$ composites at cryogenic and elevated temperatures. *Mater. Sci. Eng. A* **1996**, *206*, 183–193. [CrossRef]

30. Han, N.L.; Wang, Z.G.; Zhang, G.D. Effect of reinforcement size on the elevated-temperature tensile properties and low-cycle fatigue behavior of particulate SiC/Al composites. *Compos. Sci. Technol.* **1997**, *57*, 1491–1499. [CrossRef]

31. Vogelsang, M.; Aresenault, R.J.; Fisher, R.M. An In Situ HVEM Study of Dislocation Generation at Al/SiC Interfaces in Metal Matrix Composites. *Metall. Trans. A* **1986**, *17A*, 379–389. [CrossRef]

32. Knowles, A.J.; Jiang, X.; Galano, M.; Audebert, F. Microstructure and mechanical properties of 6061 Al alloy based composites with SiC nanoparticles. *J. Alloys Compd.* **2014**, *615*, 401–405. [CrossRef]

33. Uematsu, Y.; Tokaji, K.; Kawamura, M. Fatigue behaviour of SiC-particulate-reinforced aluminium alloy composites with different particle sizes at elevated temperatures. *Compos. Sci. Technol.* **2008**, *68*, 2785–2791. [CrossRef]

34. Biermann, H.; Kemnitzer, M.; Hartmann, O. On the temperature dependence of the fatigue and damage behaviour of a particulate-reinforced metal-matrix composite. *Mater. Sci. Eng. A* **2001**, *319–321*, 671–674. [CrossRef]

35. Vyletel, G.M.; Allison, J.E.; Van, D.C.A. The effect of matrix microstructure on cyclic response and fatigue behavior of particle—Reinforced 2219 aluminum: Part I. room temperature behavior. *Metall. Mater. Trans. A* **1995**, *26*, 3143–3154. [CrossRef]

36. Nieh, T.G.; Lesuer, D.R.; Syn, C.K. Tensile and Fatigue Properties of a 25 vol% SiC Particulate Reinforced 6090 Al Composite at 300 °C. *Scr. Metall. Mater.* **1995**, *32*, 707–712. [CrossRef]

37. Li, C.; Ellyin, F. Fatigue damage and its localization in particulate metal matrix composites. *Mater. Sci. Eng. A* **1996**, *214*, 115–121. [CrossRef]